Title

A genetically engineered neuronal membrane-based nanotoxoid elicits protective immunity against neurotoxins.

Authors

Zhu, Audrey

Wei, Xiaoli

Jiang, Yao

et al.

Publication Date

2024-08-01

DOI

10.1016/j.bioactmat.2024.05.006

Bioactive Materials 38 (2024) 321–330

Contents lists available at ScienceDirect

Bioactive Materials

journal homepage: www.keaipublishing.com/en/journals/bioactive-materials

A genetically engineered neuronal membrane-based nanotoxoid elicits protective immunity against neurotoxins

Zhongyuan Guo [a], Audrey T. Zhu [a], Xiaoli Wei [a], Yao Jiang [a], Yiyan Yu [a], Ilkoo Noh [a], Weiwei Gao [a], Ronnie H. Fang [a,b,**], Liangfang Zhang [a,*]

[a] Department of NanoEngineering, Chemical Engineering Program, Shu and K.C. Chien and Peter Farrell Collaboratory, University of California San Diego, La Jolla, CA, 92093, USA

[b] Division of Host-Microbe Systems and Therapeutics, Department of Pediatrics, University of California San Diego, La Jolla, CA, 92093, USA

ARTICLE INFO

Keywords:
Antivirulence vaccine
Cell membrane-coated nanoparticle
Genetic engineering
α-bungarotoxin
Nanotoxoid

ABSTRACT

Given their dangerous effects on the nervous system, neurotoxins represent a significant threat to public health. Various therapeutic approaches, including chelating agents, receptor decoys, and toxin-neutralizing antibodies, have been explored. While prophylactic vaccines are desirable, it is oftentimes difficult to effectively balance their safety and efficacy given the highly dangerous nature of neurotoxins. To address this, we report here on a nanovaccine against neurotoxins that leverages the detoxifying properties of cell membrane-coated nanoparticles. A genetically modified cell line with constitutive overexpression of the α7 nicotinic acetylcholine receptor is developed as a membrane source to generate biomimetic nanoparticles that can effectively and irreversibly bind to α-bungarotoxin, a model neurotoxin. This abrogates the biological activity of the toxin, enabling the resulting nanotoxoid to be safely delivered into the body and processed by the immune system. When co-administered with an immunological adjuvant, a strong humoral response against α-bungarotoxin is generated that protects vaccinated mice against a lethal dose of the toxin. Overall, this work highlights the potential of using genetic modification strategies to develop nanotoxoid formulations against various biological threats.

1. Introduction

Due to their harmful effects on the nervous system, neurotoxins are recognized to be among the deadliest toxins [1,2]. Many types of treatments have been developed to counteract their harmful effects, including chelating agents like ethylenediaminetetraacetic acid [3], receptor decoys [4], substrate analogues of enzyme toxins [5], and toxin-neutralizing antibodies [6]. However, considerable efforts are required to develop individual antitoxin treatments before they can be utilized for treating patients, and concerns such as side effects, limited availability, and suboptimal effectiveness oftentimes remain unaddressed [7]. In view of these challenges, the use of vaccines has been explored as a safe and effective alternative to protect against neurotoxins, particularly for high-risk individuals [8]. One such example of this approach is the tetanus toxoid vaccine [9], which is formulated using formalin-inactivated tetanus toxin and has been shown to offer long-lasting protection in those who are fully vaccinated [10]. Although this formulation has been approved for clinical use, the majority of neurotoxins do not have a corresponding vaccine that is available for humans [11,12]. To promote the development of such prophylactics, straightforward methods to produce vaccines that are both efficacious and safe are in great demand [13].

Compared with traditional vaccine formulations, nanovaccines that leverage various nanoparticle technologies for antigen delivery have emerged as promising alternatives. These platforms excel at eliciting immune responses due to their enhanced lymph node targeting and ability to improve delivery of antigenic material to antigen-presenting cells [14]. Among the diverse range of nanoplatforms that are actively being explored, cell membrane-coated nanoparticles have generated considerable interest due to their unique cell-mimicking properties

Peer review under responsibility of KeAi Communications Co., Ltd.

* Corresponding author. Department of NanoEngineering, Chemical Engineering Program, Shu and K.C. Chien and Peter Farrell Collaboratory, University of California San Diego, La Jolla, CA, 92093, USA.

** Corresponding author.

E-mail addresses: rhfang@ucsd.edu (R.H. Fang), zhang@ucsd.edu (L. Zhang).

https://doi.org/10.1016/j.bioactmat.2024.05.006

Received 7 January 2024; Received in revised form 2 May 2024; Accepted 3 May 2024

[15–19]. Based on their ability to interact strongly with various biological substrates [20–22], cell membrane-coated nanoparticles have been utilized as cellular nanosponges to bind and neutralize toxins such as α-hemolysin secreted by methicillin-resistant *Staphylococcus aureus* [23–25] and tetrodotoxin produced by certain marine organisms [26]. After irreversible binding with cellular nanosponges, neutralized toxins are safe to administer in vivo while still preserving their immunogenicity, a task that is difficult to accomplish using traditional heat or chemical denaturation methods [27]. These complexes, which are termed nanotoxoids, have been successful in eliciting potent immunity against a range of bacterial infections [13,28–31].

Based on their tropism to neurons [32], it has been demonstrated that neurotoxins can be effectively neutralized using neuronal cell membrane-based nanosponges [26]. While effective, detoxification using wild-type neuronal nanosponges can be insufficient due to limited expression of the appropriate receptors [33]. To enhance the binding capacity of neuronal nanosponges, it is possible to utilize genetic engineering approaches to increase the expression of specific surface receptors [34,35]. Here, we developed genetically engineered nanotoxoids as a safe and effective platform for vaccination against neurotoxins (Fig. 1). α-bungarotoxin (αBgt), which is derived from the venom of elapid snakes [36], was chosen as a model neurotoxin. Neuro-2a, a mouse neuroblastoma cell line [37], was engineered to overexpress the α7 nicotinic acetylcholine receptor (α7 nAChR), which is targeted by αBgt with high affinity [38]. The membrane from these engineered Neuro-2a cells was then coated onto a poly(lactic-*co*-glycolic acid) (PLGA) nanoparticle substrate, after which it was complexed with αBgt to produce the final nanotoxoid formulation. When administered into mice along with CpG 1826 as an adjuvant, strong antibody responses were elicited against αBgt, offering enhanced protection against subsequent toxin challenge.

2. Results and discussion

2.1. Preparation of genetically engineered α7-expressing Neuro-2a cells (α7-Neuro-2a)

According to published reports, two chaperone proteins, namely novel nAChR regulator (NACHO, encoded by *TMEM35*) and resistance to inhibitors of cholinesterase-3 (RIC-3, encoded by *RIC3*), have been shown to play crucial roles in the assembly and surface expression of α7 nAChR (encoded by *CHRNA7*) [39,40]. Wild-type Neuro-2a cells with limited α7 nAChR expression were first co-transfected with a green fluorescent protein (GFP)-tagged *CHRNA7* plasmid and a *RIC3* plasmid to construct a cell line denoted C/R-Neuro-2a. These cells were subsequently transfected with a *TMEM35* plasmid to obtain the final α7-Neuro-2a cell line. Western blotting confirmed that wild-type Neuro-2a had a low baseline expression of α7 nAChR; production was enhanced on C/R-Neuro-2a and further elevated on α7-Neuro-2a (Fig. 2a and b). Glyceraldehyde-3-phosphate dehydrogenase (GAPDH) was employed as an internal reference. To confirm the surface expression of α7 nAChR, wild-type and engineered Neuro-2a cells were analyzed by flow cytometry. As expected, α7-Neuro-2a cells showed elevated levels of surface α7 nAChR, along with its GFP tag, compared with wild-type cells, which exhibited a low level of expression over the isotype baseline (Fig. 2c–e). Next, the degree of binding between

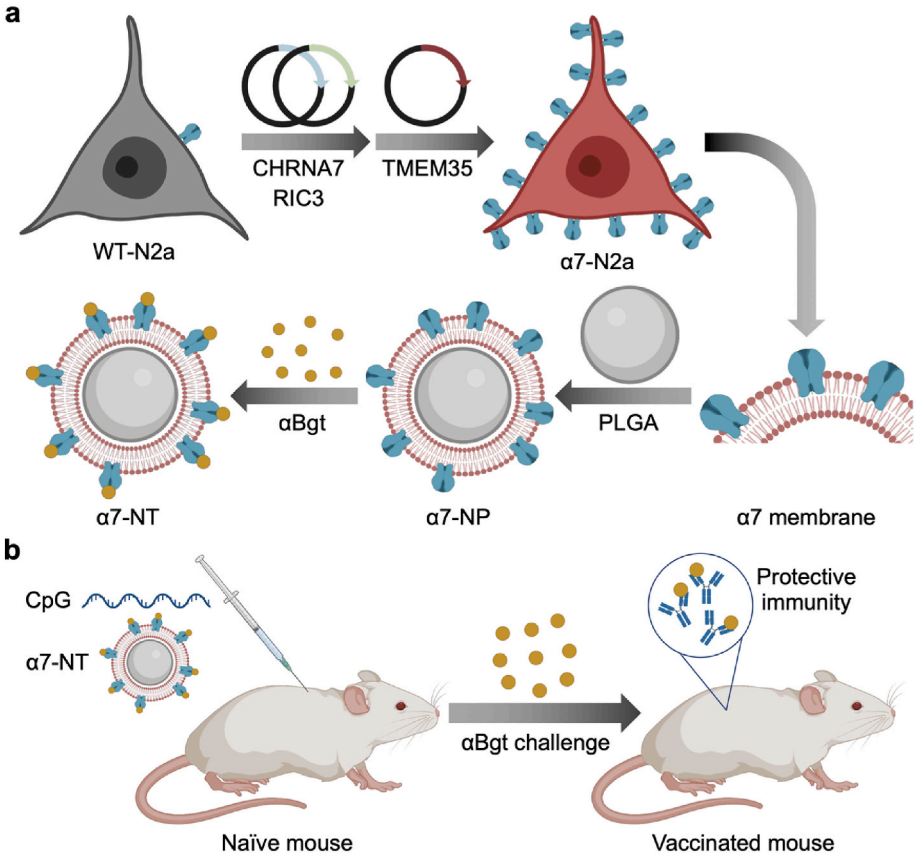

Fig. 1. Genetically engineered nanotoxoids for vaccination against neurotoxins. a) Wild-type Neuro-2a (WT-N2a) cells are modified with a combination of CHRNA7, RIC3, and TMEM35 to obtain an engineered cell line (α7-N2a) with constitutively high expression of the α7 nicotinic acetylcholine receptor (nAChR). The cell membrane derived from α7-N2a cells is coated onto a PLGA core, enabling the resulting α7-expressing nanoparticle (α7-NP) to capture and neutralize α-bungarotoxin (αBgt). b) The toxin–nanoparticle complex serves as a nanotoxoid (α7-NT) that can be used as a vaccine to elicit antibodies for protection against αBgt challenge. Created with Biorender.

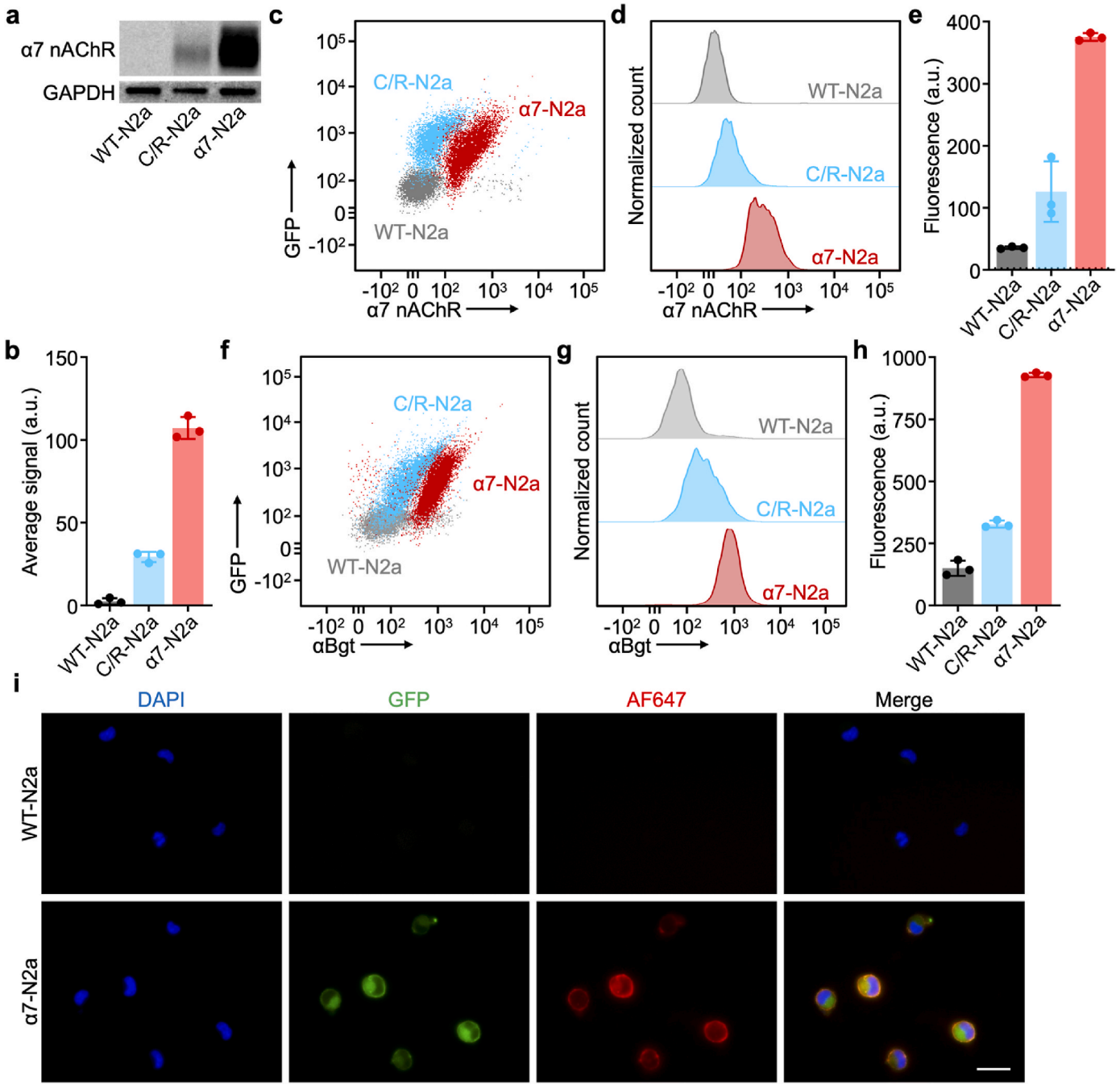

Fig. 2. Characterization of genetically engineered Neuro-2a cells. a) Representative western blot probing for α7 nAChR on WT-N2a, C/R-Neuro-2a (C/R-N2a), and α7-N2a cells. GAPDH was used as an internal reference. b) Quantification of western blots probing for α7 nAChR on WT-N2a, C/R-N2a, and α7-N2a cells (n = 3, mean ± SD). c) Representative scatter plots showing the surface expression of α7 nAChR versus signal from its GFP tag on WT-N2a, C/R-N2a, and α7-N2a cells. d,e) Representative histograms (d) and quantitative analysis (e) of the surface expression of α7 nAChR on WT-N2a, C/R-N2a, and α7-N2a cells (n = 3, mean ± SD). Dashed line: isotype control. f) Representative scatter plots showing the surface binding of αBgt versus signal from the GFP tag fused to α7 nAChR on WT-N2a, C/R-N2a, and α7-N2a cells. g,h) Representative histograms (g) and quantitative analysis (h) of the surface binding of αBgt on WT-N2a, C/R-N2a, and α7-N2a cells. i) Fluorescence images of WT-N2a and α7-N2a cells after incubation with dye-labeled αBgt. DAPI: nuclei, GFP: GFP-tagged α7 nAChR, AF647: αBgt. Scale bar = 50 μm.

dye-labeled αBgt and wild-type or engineered Neuro-2a cells was detected using flow cytometry. The results correlated well with the expression of α7 nAChR, with the engineered Neuro-2a cells binding considerably more toxin than the wild-type cells (Fig. 2f–h). The enhanced binding was further confirmed visually by fluorescence microscopy, with strong signal observed on the membrane of α7-Neuro-2a cells, whereas little signal was observed for the wild-type cells (Fig. 2i). As a result of their high αBgt binding properties while still retaining normal growth kinetics, we chose to employ α7-Neuro-2a for all subsequent studies.

2.2. Construction and characterization of α7-expressing nanoparticles (α7-NPs)

After confirming the improved expression of α7 nAChR and the increased αBgt binding for α7-Neuro-2a cells, we next derived their plasma membrane and coated it onto preformed nanoscale PLGA cores using a sonication process [41]. To optimize the preparation of α7-NPs,

different weight ratios of α7-Neuro-2a membrane to PLGA were evaluated. After nanoparticle fabrication, changes in size after transferring to phosphate buffered saline (PBS) were determined (Fig. 3a). The nanoparticles were relatively stable in PBS down to a 1:2 wt ratio of cell membrane to PLGA, which we selected for subsequent α7-NP preparation. Western blotting was performed to detect for α7 nAChR on protein-normalized cell lysate, cell membrane, and cell membrane-coated nanoparticle samples derived from either wild-type Neuro-2a or α7-Neuro-2a cells (Fig. 3b). While nothing was detected in the wild-type samples, all samples derived from α7-Neuro-2a cells showed strong banding. This confirmed that, following the entire fabrication process, α7 nAChR was successfully transferred from the genetically engineered cells onto the PLGA nanoparticle cores.

To investigate the binding of cell membrane-coated nanoparticles fabricated using wild-type Neuro-2a membrane (WT-NPs) and α7-NPs to αBgt, the nanoparticles were first incubated at different weight ratios with dye-labeled toxin, followed by separation using size exclusion chromatography (Fig. 3c). Binding efficiency was calculated as the percentage of fluorescent signal coinciding with the nanoparticle fractions out of the total inputted signal. Binding efficiency initially increased with increasing α7-NP to αBgt ratios, plateauing at a ratio of 10000:1. When incubating with WT-NPs, αBgt binding saturated considerably faster at a 2000:1 ratio. A ratio of 10000:1 was chosen for subsequent nanotoxoid fabrication. The submaximal binding efficiency of α7-NPs at saturation is likely an artifact of the fluorescent labeling of αBgt, and this may be overcome in the future by using analytical techniques such as mass spectrometry. As it has been reported that αBgt can inhibit nicotine-induced calcium flux [42,43], we elected to further evaluate the impact of nanoparticle complexation on the activity of the toxin. α7-Neuro-2a cells were treated with αBgt, either in free form or preincubated with WT-NPs or α7-NPs, followed by exposure to nicotine, and intracellular calcium was monitored using a fluorescent probe (Fig. 3d). As a baseline, exposure to nicotine only without any pretreatment resulted in approximately a 50 % signal increase. Whereas the response to nicotine was significantly dampened in the presence of free αBgt, preincubation with α7-NPs abrogated this inhibitory effect. Preincubation with WT-NPs did not restore the response of the cells to nicotine. It was also confirmed that neither WT-NPs nor α7-NPs impacted the normal response of the cells to nicotine exposure. These results confirmed that α7-NPs could not only bind to αBgt, but the nanoparticles also effectively neutralized the activity of the toxin.

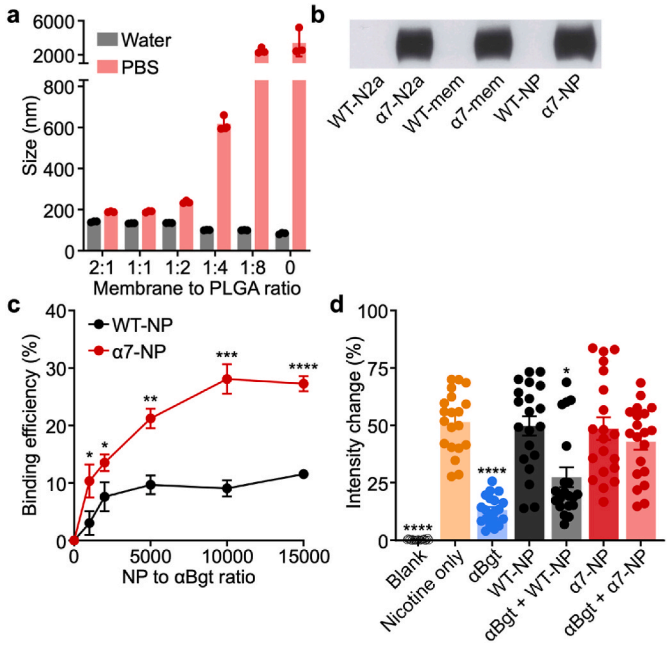

Fig. 3. Characterization of α7-NPs. a) Size of α7-NPs fabricated at different membrane to PLGA weight ratios in water and after adjusting to 1 × PBS (n = 3, mean ± SD). b) Representative western blot probing for α7 nAChR on cell lysate, cell membrane, and cell membrane-coated nanoparticle samples derived from WT-N2a and α7-N2a cells. c) Binding efficiency of αBgt to WT-NPs or α7-NPs at different nanoparticle (NP) to toxin weight ratios (n = 3, mean ± SD). $^{*}p < 0.05$, $^{**}p < 0.01$, $^{***}p < 0.001$, $^{****}p < 0.0001$, Student's *t*-test. d) Nicotine-induced calcium flux as indicated by Fluo-4 AM signal in α7-N2a cells after treatment with free αBgt, WT-NPs, α7-NPs, and αBgt preincubated with WT-NPs or α7-NPs (n = 20, mean ± SEM). Untreated cells and cells treated with nicotine only were employed as controls. $^{*}p < 0.05$ and $^{****}p < 0.0001$ (compared to αBgt + α7-NP), one-way ANOVA with Tukey's multiple comparisons test.

2.3. Characterization of nanotoxoids constructed using α7-NPs (α7-NTs)

After confirming the successful incorporation of αBgt with α7-NPs, we utilized the resulting nanocomplexes as α7-NTs. The size of the final formulation was approximately 100 nm, representing a slight increase from the bare PLGA cores (Fig. 4a). The surface zeta potential of the α7-NTs was similar to that of α7-Neuro-2a cell membrane, suggesting that the coating process was successful (Fig. 4b). The size of α7-NTs remained stable when stored at 4 °C for at least 4 weeks (Fig. 4c). Using transmission electron microscopy, it was observed that α7-NTs exhibited a spherical core–shell structure, which is characteristic of cell membrane-coated nanoparticles (Fig. 4d) [30,44]. To explore the impact of nanoparticle complexation on the uptake of αBgt, dye-labeled toxin was incubated with DC2.4 dendritic cells either in free form or as part of the α7-NT formulation (Fig. 4e–g). Whereas free αBgt experienced almost no uptake by DC2.4 cells, internalization was elevated considerably when the toxin was incorporated into α7-NTs, and uptake increased rapidly for the first several hours before leveling off around 16 h. The potential toxicity of α7-NTs was evaluated in vitro, and the formulation was found to be safe when incubated with wild-type Neuro-2a cells (Fig. 4h).

2.4. In vivo characterization and efficacy of α7-NTs

In order to effectively elicit adaptive immune responses, vaccine antigens need to be transported via the lymphatic system to the lymph nodes after administration and processed by antigen-presenting cells. To explore time-dependent lymph node drainage, dye-labeled α7-NTs were injected subcutaneously at the hock site, and the draining popliteal lymph nodes were collected at 6 h and 24 h after injection (Fig. 5a and b). The results clearly demonstrated that α7-NTs could be transferred to the draining lymph nodes one day after administration. We further investigated the cell population-specific uptake of α7-NTs in the lymph nodes (Fig. 5c). At 24 h, professional antigen-presenting cells such as B cells, macrophages, and dendritic cells were associated with the highest degree of α7-NT signal. Based on the subcutaneous route of administration, it could be inferred that systemic exposure to α7-NTs was limited [45].

To elicit strong antibody titer responses against αBgt, α7-NTs were co-administered with the Toll-like receptor 9 agonist CpG 1826 as an adjuvant. Mice were vaccinated subcutaneously once every week for a total of 3 doses on days 0, 7 and 14. As a control, mice were vaccinated with the same dose of heat-inactivated αBgt (iαBgt) adjuvanted with CpG 1826. Serum IgG titers against αBgt were monitored over time (Fig. 5d and e). On day 7 after the first vaccination, mice from both vaccinated groups had similar titers compared to the naïve group. On day 21 after the first vaccination, αBgt-specific titers became significantly elevated for mice receiving α7-NTs with CpG 1826, whereas the levels for mice receiving iαBgt with CpG 1826 remained consistent with the naïve group. It was also determined that lowest dose of αBgt required to elicit a response using α7-NTs was 100 ng (Fig. 5f).

Protective efficacy was evaluated on day 22 in a survival model commonly used to evaluate immunization strategies against snake toxins [46]. All mice were challenged with a lethal dose of αBgt (Fig. 5g).

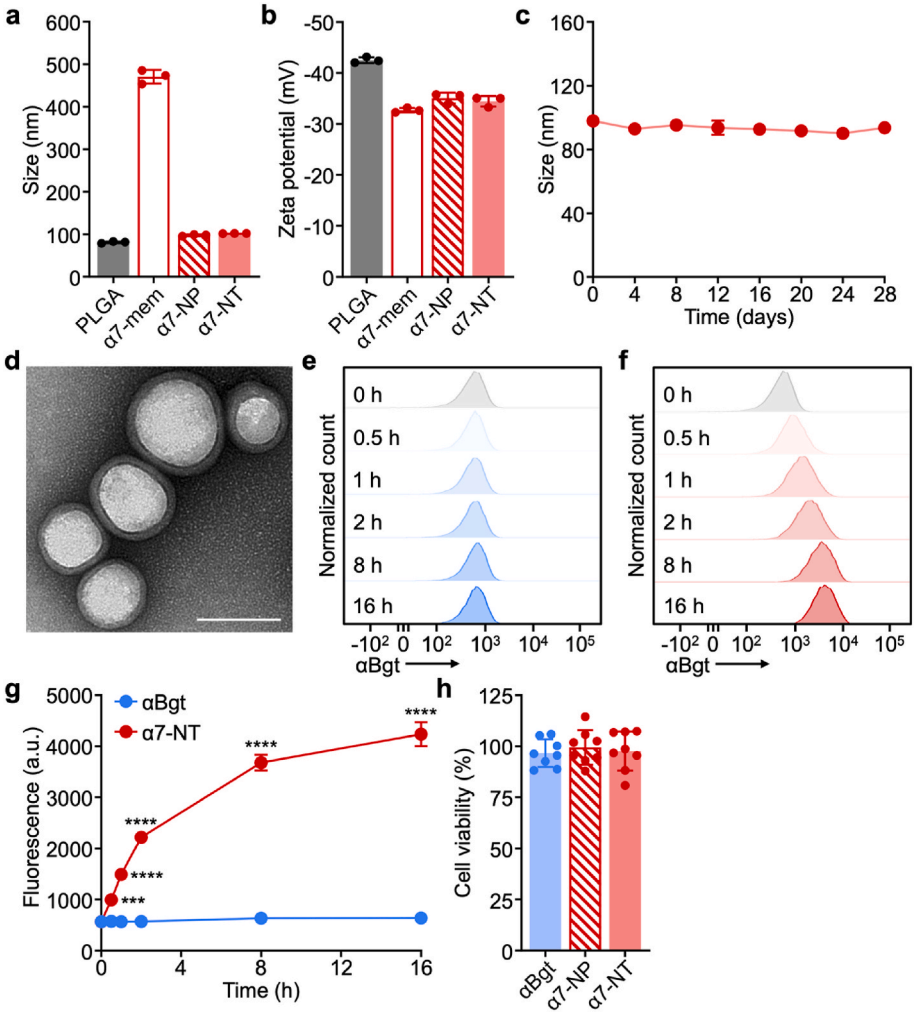

Fig. 4. Characterization of α7-NTs. a,b) Size (a) and zeta potential (b) of bare PLGA cores, α7-N2a membrane, α7-NPs, and α7-NTs (n = 3, mean ± SD). c) Size over time of α7-NTs stored in water at 4 °C (n = 3, mean ± SD). d) Transmission electron microscopy image of α7-NTs negatively stained with uranyl acetate. Scale bar = 100 nm. e,f) Representative histograms showing the cellular uptake of dye-labeled αBgt in free form (e) and on α7-NTs (f). g) Quantification of cellular uptake of dye-labeled αBgt in free form and on α7-NTs (n = 3, mean ± SD). ***$p < 0.001$ and ****$p < 0.0001$, Student's *t*-test. (h) Viability of WT-N2a cells treated with free αBgt, α7-NPs, or α7-NTs (n = 8, mean ± SD).

Vaccination with α7-NTs and CpG 1826 significantly prolonged the median survival time from 1 h for the two control groups to 18 h, and 25 % of the mice survived long-term. To assess the safety profile of the vaccine formulations, we immunized healthy mice and collected blood and serum samples after 24 h. All blood chemistry parameters and cell counts were consistent with those of control mice (Fig. 5h and i).

2.5. Cellular immune responses to α7-NTs

To evaluate antigen-specific adaptive T cell responses, splenocytes from vaccinated mice were collected and restimulated with αBgt. The secretion of cytokines, including interferon γ (IFNγ), interleukin 4 (IL4), and IL17A, was evaluated (Fig. 6a–c). Only the production of IL4 was elevated in samples from mice receiving iαBgt with CpG 1826, whereas both IL4 and IFNγ were elevated in the group that received α7-NTs with CpG 1826. This indicated that the α7-NTs were superior at eliciting a T helper 1-biased immune response. Neither vaccine formulation was able to promote the production of IL17A upon restimulation. Similar trends were observed when analyzing for the same cytokines in $CD4^+$ T cells by intracellular staining using flow cytometry (Fig. 6d–f). Additionally, we assayed for the presence of memory B cells 21 days after vaccination. In this case, only α7-NTs with CpG 1826 elevated the number of cells with the appropriate $CD19^+CD73^+$ phenotype in the draining lymph nodes (Fig. 6g).

3. Conclusions

In conclusion, we have developed an effective nanovaccine formulation designed to elicit robust humoral immunity against αBgt. Wild-type Neuro-2a cells were genetically engineered for high expression of α7 nAChR. After collecting the membrane of the engineered cells and coating it onto the surface of nanoscale PLGA cores, the resulting cell membrane-coated nanoparticles were able to irreversibly bind αBgt. This nanoparticle detainment led to the neutralization of the toxin's biological activity, making it safe to administer in vivo. When co-administered with the adjuvant CpG 1826, elevated αBgt-specific IgG titers were generated, which subsequently helped to protect mice against a lethal toxin challenge. This work demonstrates that using genetic engineering to upregulate specific cellular receptors is a viable method for generating nanotoxoids with enhanced antigen loading; future formulations could also be genetically manipulated to reduce unwanted immunogenicity [47]. Overall, this will enable the effective design of a diverse range of cell membrane-based nanovaccines beyond what is possible using wild-type source cells.

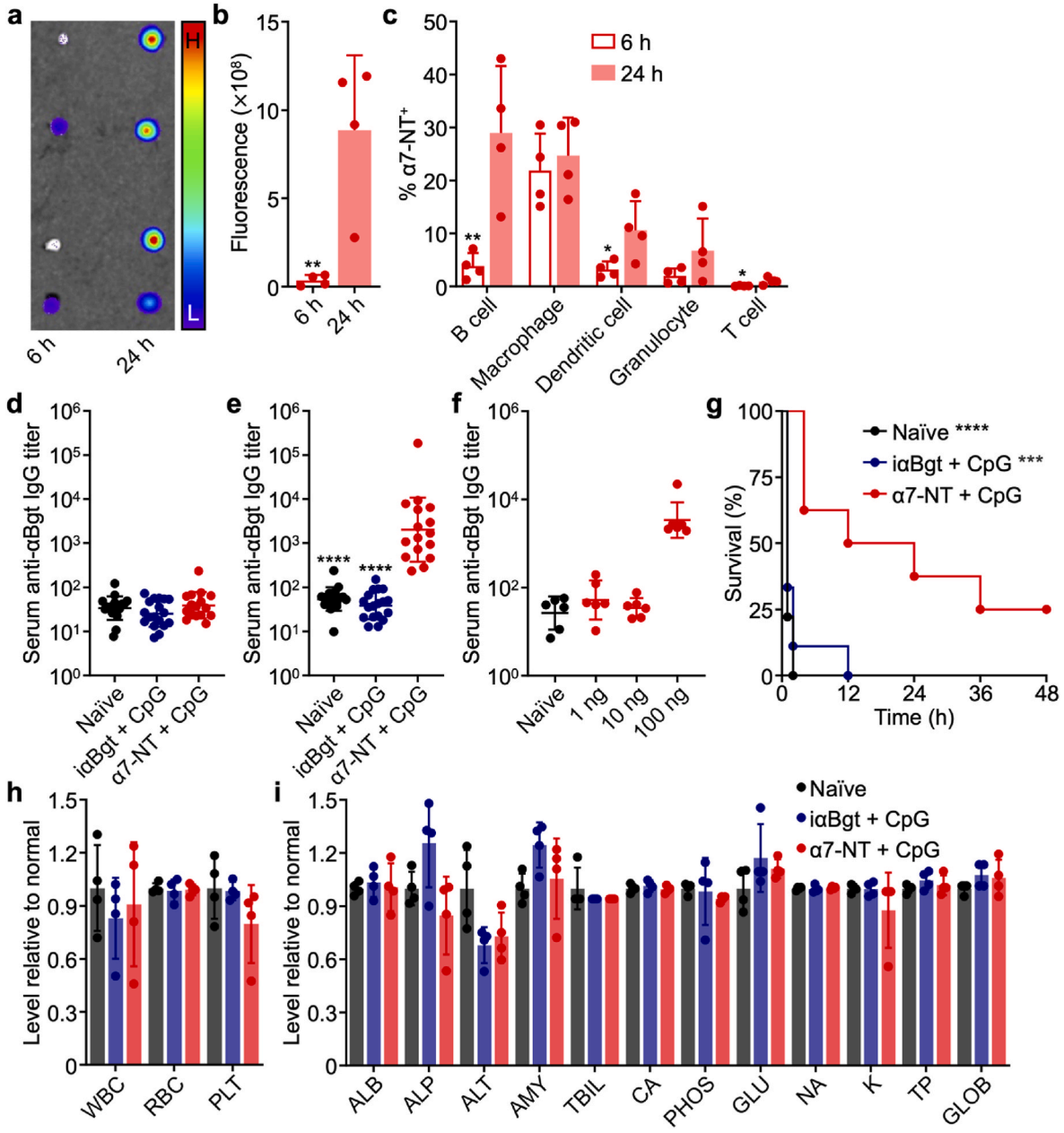

Fig. 5. In vivo transport, titers, prophylactic efficacy, and safety. a,b) Fluorescent imaging (a) and quantitative analysis (b) of dye-labeled α7-NT uptake in the draining lymph node at 6 h and 24 h after subcutaneous administration (n = 4, mean ± SD). H: high signal, L: low signal. $^{**}p < 0.01$, Student's unpaired *t*-test. c) Percentage of cells positive for α7-NT uptake among various populations in the draining lymph nodes at 6 h and 24 h after subcutaneous administration (n = 4, mean ± SD). $^{*}p < 0.05$ and $^{**}p < 0.01$, Student's unpaired *t*-test. d,e) Serum αBgt-specific IgG titers on day 7 (d) and day 21 (e) during the course of vaccination with heat-inactivated αBgt (iαBgt) and α7-NT (both adjuvanted with CpG 1826) on days 0, 7, and 14 (n = 16 for α7-NT + CpG, n = 18 for naïve and iαBgt + CpG, geometric mean ± SD). $^{****}p < 0.0001$ (compared to α7-NT + CpG), one-way ANOVA with Tukey's multiple comparisons test. f) Serum αBgt-specific IgG titers on day 21 after vaccination with α7-NT adjuvanted with CpG 1826 on days 0, 7, and 14 at αBgt dosages of 1, 10, and 100 ng (n = 6, geometric mean ± SD). g) Survival of mice vaccinated with iαBgt and α7-NT (both adjuvanted with CpG 1826) after challenge with a lethal dose of αBgt (n = 8 for α7-NT + CpG, n = 9 for naïve and iαBgt + CpG). $^{***}p < 0.001$ and $^{****}p < 0.0001$, Mantel–Cox test. h,i) Blood cell counts (h) and serum chemistry parameters (i) analyzed 24 h after subcutaneous administration of iαBgt and α7-NT (both adjuvanted with CpG 1826) (n = 4, mean ± SD). WBC: white blood cell, RBC: red blood cell, PLT: platelet; ALB: albumin, ALP: alkaline phosphatase, ALT: alanine transaminase, AMY: amylase, TBIL: total bilirubin, CA: calcium, PHOS: phosphorus, GLU: glucose, NA: sodium, K: potassium, TP: total protein, GLOB: globulin (calculated).

4. Materials and methods

4.1. Animal care

Six-week-old male CD1 mice were purchased from Envigo and housed in an animal facility at Moores Cancer Center at the University of California San Diego (UCSD). All animal experiments were performed under federal, state, and local regulations in accordance with National Institutes of Health guidelines and approved by the Institutional Animal Care and Use Committee of UCSD.

4.2. Genetic engineering of Neuro-2a cells

Wild-type Neuro-2a mouse neuroblastoma cells (CCL-131, American

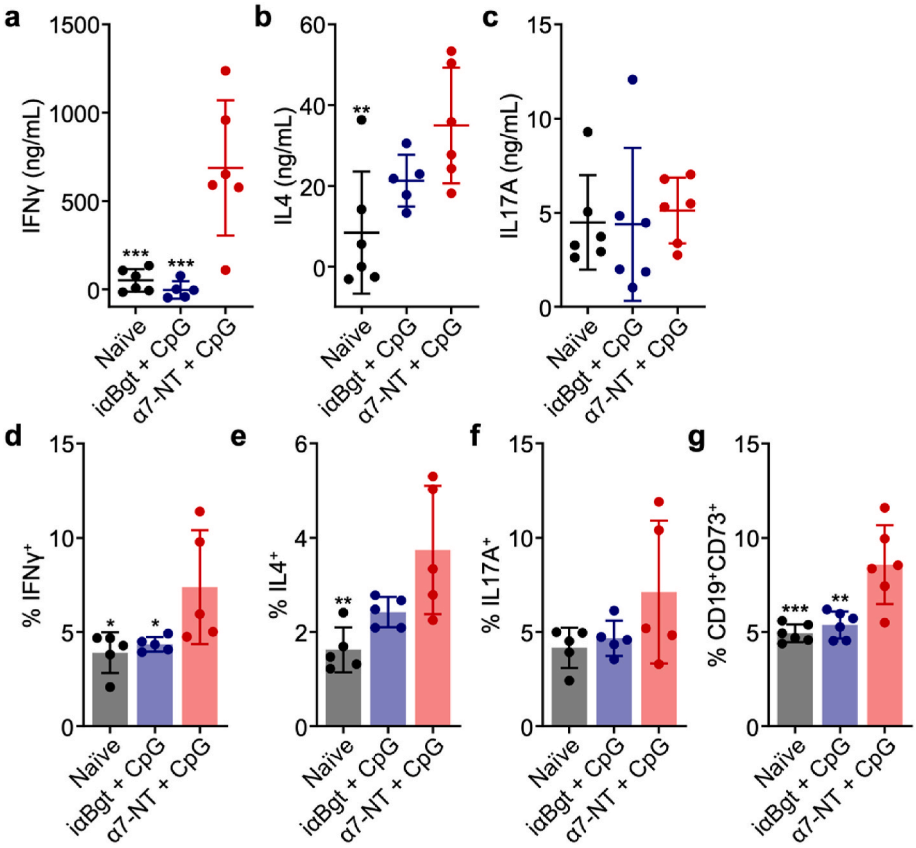

Fig. 6. Cellular immune responses. a-c) Secretion of IFNγ (a), IL4 (b), and IL17A (c) by splenocytes collected from mice vaccinated with iαBgt and α7-NT (both adjuvanted with CpG 1826) on days 0, 7, and 14, followed by restimulation with αBgt for 5 days (n = 6, mean ± SD). d-f) Expression of IFNγ (d), IL4 (e), and IL17A (f) by $CD3^+CD4^+$ splenocytes collected from mice vaccinated with iαBgt and α7-NT (both adjuvanted with CpG 1826) on days 0, 7, and 14, followed by restimulation with αBgt for 4 h (n = 5, mean ± SD). g) Cells with the $CD19^+CD73^+$ phenotype in the draining lymph nodes of mice 21 days after vaccination with iαBgt and α7-NT (both adjuvanted with CpG 1826) on days 0, 7, and 14 (n = 6, mean ± SD). *$p < 0.05$, **$p < 0.01$, and ***$p < 0.001$, one-way ANOVA with Dunnett's multiple comparisons test.

Type Culture Collection) were cultured in Dulbecco's modified Eagle's medium (DMEM; Corning) supplemented with 10 % fetal bovine serum (FBS; Gibco) and 1 % penicillin–streptomycin (Gibco). To overexpress α7 nicotinic acetylcholine receptor (nAChR) on the cell surface, wild-type Neuro-2a cells were first co-transfected with plasmids encoding for α7 nAChR (pcDNA3.1-CHRNA7-mGFP, a gift from Henry Lester, Addgene #62629) and RIC-3 (pcDNA3.1$^+$/C-(K)-DYK-RIC3, Genscript) using Lipofectamine 2000 (Invitrogen). The transfected Neuro-2a cells were cultured in selection medium containing 200 μg/mL of hygromycin B (InvivoGen) and 800 μg/mL of G418 (InvivoGen) and sorted for high green fluorescent protein (GFP) expression and high binding to Alexa Fluor 647-labeled α-bungarotoxin (αBgt) (Invitrogen). For sorting, transfected cells were collected using 1 mM ethylenediaminetetraacetic acid (EDTA; Invitrogen) and blocked with 10 % FBS in phosphate-buffered saline (PBS; Corning) for 30 min on ice to reduce nonspecific binding. The cells were then stained with Alexa Fluor 647-labeled αBgt at a ratio of 1 μg per million cells and processed by flow cytometry using a Becton Dickinson FACSAria. Monoclonal selection by limiting dilution was performed to obtain an initial engineered Neuro-2a cell line with constitutively high α7 nAChR expression (C/R-Neuro-2a). To further enhance the surface expression of α7 nAChR, C/R-Neuro-2a cells were transfected with a plasmid encoding for TMEM35, which was generated by subcloning the *TMEM35* gene (pcDNA3.1$^+$/C-(K)-DYK-TMEM35a, Genscript) into a pUNO1 backbone (InvivoGen). The transfected cells were cultured in selection media containing 200 μg/mL hygromycin B, 200 μg/mL G418, and 10 μg/mL blasticidin (InvivoGen), followed by another round of sorting to obtain the final cell line with the highest α7 nAChR expression (α7-Neuro-2a).

4.3. Preparation of cell membrane-coated nanoparticles

The plasma membrane of wild-type Neuro-2a or α7-Neuro-2a cells was derived following a previous protocol with minor modifications [30]. Briefly, cells were washed 3 times in 30 mM Tris-HCl buffer at pH 7.5 (Quality Biological) containing 225 mM D-mannitol (Sigma-Aldrich) and 76 mM sucrose (Sigma-Aldrich). Afterwards, the cells were resuspended in the same buffer supplemented with a phosphatase inhibitor cocktail (Sigma-Aldrich) and a protease inhibitor cocktail (Sigma-Aldrich), followed by disruption with a Kinematica Polytron PT 10/35 probe homogenizer at 70 % power for 20 passes. The cell homogenate was centrifuged at 10,000 *g* for 25 min, after which the supernatant was collected and spun down twice at 150,000 *g* for 35 min to pellet the membrane material using a Beckman Coulter Optima XPN-80 ultracentrifuge. The membrane was suspended in 0.2 mM EDTA in water at a protein concentration of 5 mg/mL and stored at −80 °C for further use. To prepare nanoparticle cores, 0.66 dL/g carboxyl-terminated poly (lactic-*co*-glycolic acid) (PLGA, LACTEL Absorbable Polymers) was dissolved in acetone to a concentration of 10 mg/mL. A volume of 1 mL of the polymer was injected into 2 mL of water, and the organic solvent was evaporated under vacuum for 2 h. For dye labeling, 0.1 wt% 1,1′-dioctadecyl-3,3,3′,3′-tetramethylindodicarbocyanine, 4-chlorobenzenesulfonate salt (DiD; excitation/emission = 644/665 nm, Invitrogen) was premixed with the PLGA in acetone prior to injection into water. For coating, the PLGA cores and cell membrane were mixed together at the prescribed polymer to membrane protein weight ratios and sonicated for 2 min using a Fisher Scientific FS30D bath sonicator.

4.4. Western blotting to detect α7 nAChR

Wild-type Neuro-2a, C/R-Neuro-2a, and α7-Neuro-2a cells were collected and lysed in water using a Fisher Scientific FS30D bath sonicator. For all cell lysate, cell membrane, and cell membrane-coated nanoparticle samples, protein concentrations were determined using a Pierce BCA protein assay kit (Thermo Scientific), followed by normalization to a protein concentration of 0.4 mg/mL. The samples were then prepared using 4 × NuPAGE LDS sample buffer (Invitrogen), heated at 70 °C for 10 min, loaded into Bolt 4–12 % Bis-Tris plus gels (Invitrogen), and run at 165 V for 45 min in NuPAGE MOPS SDS running buffer (Invitrogen). Transfer onto nitrocellulose membrane (Thermo Scientific) was performed in Bolt transfer buffer (Invitrogen) at 15 V for 30 min. The blots were blocked with 1 % bovine serum albumin (BSA; Sigma-Aldrich) and 5 % nonfat dry milk (Apex) in PBS containing 0.05 % Tween 20 (National Scientific) for 1 h at room temperature, followed by incubation for 16 h at 4 °C with a rabbit polyclonal anti-CHRNA7 (21379-1-AP, Proteintech) or a rat monoclonal anti-GAPDH (W17079A, BioLegend). An appropriate horseradish peroxidase (HRP)-conjugated secondary (BioLegend) was then incubated with the membrane for 2 h at room temperature. Membranes were further developed on film using Pierce ECL western blotting substrate (Thermo Scientific).

4.5. Flow cytometry to detect α7 nAChR expression and αBgt binding

Wild-type Neuro-2a, C/R-Neuro-2a, and α7-Neuro-2a cells were collected using 1 mM EDTA in PBS and blocked using 1 % BSA in PBS on ice for 30 min. For detection of α7 nAChR, the blocked cells were stained with a rabbit polyclonal anti-CHRNA7 (PA5-115651, Invitrogen) and then an Alexa Fluor 647-labeled secondary (Poly4064, BioLegend). A rabbit polyclonal IgG control (30000-0-AP, Proteintech) was utilized as an isotype. For detection of αBgt binding, blocked cells were stained with Alexa Fluor 647-labeled αBgt. Data were collected using a Becton Dickinson LSR II flow cytometer and analyzed in FlowJo v10.4 software.

4.6. Fluorescence microscopy to image αBgt binding

Wild-type Neuro-2a and α7-Neuro-2a cells were seeded into a 4-well Nunc Lab-Tek chambered coverglass (Thermo Scientific) at a density of 50,000 cells per chamber and incubated at 37 °C for 12 h. The cells were then incubated with 30 μg/mL of Alexa Fluor 647-labeled αBgt in 2 % FBS in PBS for 15 min at 4 °C and further stained with 10 mM Hoechst 33342 (Thermo Scientific) at room temperature for 15 min. The cells were washed once with 2 % FBS in PBS and imaged under a Keyence BZ-X710 fluorescence microscope.

4.7. Preparation of nanotoxoids

α7-Neuro-2a cell membrane-coated nanoparticles (α7-NPs) were incubated with αBgt (Millipore Sigma) or Alexa Fluor 647-labeled αBgt at the prescribed polymer to αBgt weight ratios at room temperature for 2 h to prepare nanotoxoids (α7-NTs). For in vivo studies, α7-NTs were adjusted to a polymer concentration of 5 mg/mL in 10 % sucrose in water. For vaccination studies, α7-NTs were mixed with CpG 1826 (Integrated DNA Technologies) at a 20:1 polymer to DNA weight ratio right before administration. To generate a heat-inactivated αBgt (iαBgt) control, the toxin was heated at 99 °C for 12 h.

4.8. Characterization of membrane-coated nanoparticles and nanotoxoids

The size and zeta potential of nanoparticles and nanotoxoids were measured using a Malvern Zetasizer Nano ZS90. To monitor stability, α7-NTs in water were stored at 4 °C for 4 weeks, and their size was measured every 4 days. To visualize morphology, a sample of α7-NTs was negatively stained with 1 % uranyl acetate (Electron Microscopy Sciences) and imaged using a JEOL JEM-1400Plus transmission electron microscope at the Cellular and Molecular Medicine Electron Microscopy Core (UCSD-CMM-EM Core, RRID: SCR_022039).

4.9. Binding efficiency characterization

A mass of 20 ng of Alexa Fluor 647-labeled αBgt was incubated with different amounts of wild-type Neuro-2a cell membrane-coated nanoparticles (WT-NPs) and α7-NPs (20, 40, 100, 200, or 300 μg based on polymer weight) in water for 2 h at room temperature. Size-based separation was performed in columns filled with Sepharose CL-4B (Sigma-Aldrich) using 1 mM sodium acetate buffer at pH 5.2 (Sigma-Aldrich) as the eluent. Fractions were collected into 96-well clear polystyrene microplates (Corning) with 4 drops per well, and fluorescence was measured using a Tecan Spark 20M multimode microplate reader. Binding efficiency percentage was calculated as the percentage of Alexa Fluor 647 signal eluted with α7-NPs relative to the total inputted signal after background subtraction.

4.10. Inhibition of nicotine-induced calcium flux

α7-Neuro-2a cells were seeded into 96-well cell culture plates (Genesee Scientific) at a density of 10,000 cells per well and incubated at 37 °C for 16 h. The cells were then incubated with 1 mM Fluo-4 AM (Abcam) in complete DMEM medium at 37 °C for 30 min and washed once with Hanks' balanced salt solution (HBSS; Gibco). Then, free αBgt, WT-NPs, α7-NPs, WT-NPs plus αBgt, or α7-NPs plus αBgt in HBSS were added at a final αBgt concentration of 1 ng/mL or membrane protein concentration of 10 μg/mL. To prevent any nonspecific interactions for the last two groups, WT-NPs and α7-NPs were blocked with 1 % BSA at room temperature for 30 min and then incubated with αBgt at a 10,000:1 PLGA to αBgt weight ratio for 2 h at room temperature. After 30 min of incubation at 37 °C, the cells were washed 3 times with HBSS, and fluorescent images before and after the addition of 100 μL of 5 mM (−)-nicotine (Sigma-Aldrich) in HBSS were obtained using an Invitrogen EVOS FL digital inverted fluorescence microscope. For analysis using ImageJ, 20 cells were picked randomly. The intensity change percentage was calculated as the percentage increase in intensity after adding (−)-nicotine, compared to the initial intensity before adding (−)-nicotine. α7-Neuro-2a cells not exposed to nicotine or any treatment, as well as cells only exposed to nicotine, were employed as additional controls.

4.11. Cellular uptake and toxicity of α7-NTs

To detect the uptake of α7-NTs, DC2.4 dendritic cells (a gift from Dr. Dong-Er Zhang's laboratory) were seeded into 12-well cell culture plates (Genesee Scientific) at 37 °C for 16 h. Cells were treated with 60 ng/mL of free Alexa Fluor 647-labeled αBgt or an equal dose of toxin on α7-NTs and incubated at 37 °C for increasing periods of time. Data were collected using a Becton Dickinson LSR II flow cytometer and analyzed in FlowJo v10.4 software. To evaluate toxicity, wild-type Neuro-2a cells were seeded into 96-well cell culture plates (Genesee Scientific) at 37 °C for 16 h. Cells were treated with α7-NTs at an αBgt dose of 60 ng/mL and incubated at 37 °C for 24 h. Free toxin or an equivalent amount of α7-NPs were employed as controls. Cell viability was measured using a CellTiter 96 AQ_{ueous} One Solution cell proliferation assay (Promega) following the vendor's instruction.

4.12. Lymph node transport

CD1 mice were subcutaneously injected in their hock regions with DiD-labeled α7-NTs, and their draining lymph nodes were collected at 6 or 24 h after injection for imaging and quantification using a PerkinElmer Xenogen IVIS 200 imaging system. For cellular level analysis, single-cell suspensions were generated from lymph node samples by manual dissociation, passage through Flowmi 40-μm cell strainers (Bel-

Art), and 2 washes with PBS. The cell suspensions were then incubated with a LIVE/DEAD fixable aqua dead cell stain kit (Invitrogen), blocked with 1 % BSA in PBS, and stained with a panel of antibodies, including FITC anti-mouse CD3 (17A2, BioLegend), Pacific Blue anti-mouse CD19 (6D5, BioLegend), PE/cyanine7 anti-mouse CD11c (N418, BioLegend), PE anti-mouse F4/80 (BM8, BioLegend), APC/cyanine7 anti-mouse CD11b (M1/70, BioLegend), and PerCP anti-mouse Ly-6G/Ly-6C (Gr-1) (RB6-8C5, BioLegend). B cells were defined as $CD19^{+}$, macrophages were defined as $CD11b^{+}F4/80^{+}$, dendritic cells were defined as $CD11c^{+}F4/80^{-}$, granulocytes were defined as $CD11b^{+}Gr\text{-}1^{+}$, and T cells were defined as $CD3^{+}$. Unstained, single-stained controls, and fluorescence-minus-one controls were used for compensation and gating purposes. Data were acquired using a Becton Dickinson LSR II flow cytometer and analyzed using FlowJo v10.4 software.

4.13. Titer responses, prophylactic efficacy, and safety

CD1 mice were vaccinated subcutaneously in the hock on days 0, 7, and 14 with 100 ng iαBgt or 1 mg of α7-NTs loaded with 100 ng of αBgt, each supplemented with 50 μg of CpG 1826 as an adjuvant. On days 7 and 21, the sera from mice were collected for analysis by indirect ELISA. In brief, 96-well clear polystyrene microplates were coated using 2 μg/mL of αBgt in ELISA coating buffer (BioLegend) at 4 °C for 16 h, followed by blocking with 1 % BSA and 5 % nonfat dry milk in PBS containing 0.05 % Tween 20 for 1 h at room temperature. Serum samples were serially diluted in the blocking buffer and loaded onto the toxin-coated plates, followed by incubation at room temperature for 2 h. Each well was further treated with the appropriate HRP-conjugated secondary (Poly4053, BioLegend) and developed using TMB substrate (BioLegend). After stopping the reaction using 1 N hydrochloric acid, the absorbance at 450 nm was measured using a Tecan Spark 20M multimode microplate reader. The data were fitted using a four-parameter logistic curve, and titer levels were interpolated in GraphPad Prism 8. On day 22, the vaccinated mice were intravenously challenged with αBgt at a dose of 150 μg/kg, and survival was monitored over the next 2 days. For the dose-dependent titer study, α7-NTs were injected at αBgt doses of 1, 10, or 100 ng with 50 μg of CpG 1826 following the same schedule as before. On day 21, serum samples were collected to detect αBgt-specific IgG titers. To evaluate biosafety, healthy CD1 mice were injected subcutaneously with iαBgt or α7-NTs, each supplemented with CpG, at the same dosages as above. Blood and serum samples were collected after 24 h. Cell counting and complete blood chemistry analysis was conducted by the UCSD Animal Care Program Diagnostic Services Laboratory.

4.14. Cellular immune responses

For antigen-specific T cell analysis, spleens collected on day 21 from mice vaccinated as before were mechanically dissociated in sterile PBS containing 1 mg/mL of DNase I (Roche) and 1 mg/mL of collagenase D (Roche). After filtration through 70-μm cell strainers (Fisher Scientific) and red blood cell lysis using a commercial buffer (BioLegend), splenocytes were cultured at a density of 2 million cells per 1 mL of media and stimulated with αBgt at a final concentration of 1 μg/mL. For cytokine analysis, 200 μL of the media was collected after 5 days for detection by ELISA with the appropriate antibody pairs (IFNγ: XMG1.2 and R4-6A2, IL4: 11B11 and BVD6-24G2, IL17A: TC11-18H10.1 and TC11-8H4; BioLegend). For flow cytometric analysis, splenocytes were stimulated with αBgt for 4 h and then treated with 5 μg/mL of brefeldin A (BioLegend) for another 20 h. The cells were then collected with 1 mM EDTA in PBS and stained with a LIVE/DEAD fixable aqua dead cell stain kit for 30 min. Subsequently, the cells were blocked with 1 % BSA in PBS for 30 min, and further stained with Alexa Fluor 700 anti-mouse CD3 (17A2, BioLegend) and APC/Fire 750 anti-mouse CD4 (GK1.5, BioLegend) for 30 min. After treatment with a FIX & PERM cell permeabilization kit (Invitrogen), the cells were further stained intracellularly with APC anti-mouse IFNγ (XMG1.2, BioLegend), Alexa Fluor 488 anti-mouse IL4 (11B11, BioLegend), and PE anti-mouse IL17A (TC11-18H10.1, BioLegend). The cells were then washed twice and resuspended using PBS. Data was collected using a Becton Dickinson LSR II flow cytometer, and analysis was performed using FlowJo software.

To evaluate memory B cells, mice were vaccinated as before. On day 21, the axillary lymph nodes were collected, manually dissociated, and filtered through Flowmi 40-μm cell strainers to prepare single-cell suspensions. The cells were then stained with a LIVE/DEAD fixable aqua dead cell stain kit for 30 min and blocked with 1 % BSA in PBS for 30 min at 4 °C. Subsequently, the cells were stained with Pacific Blue anti-mouse CD19 and PE/cyanine7 anti-mouse CD73 (TY/11.8, BioLegend) for another 30 min at 4 °C. The cells were then washed twice and resuspended using PBS. Data was collected using a Becton Dickinson LSR II flow cytometer, and analysis was performed using FlowJo software.

Ethics approval and consent to participate

All animal experiments were performed under federal, state, and local regulations in accordance with National Institutes of Health guidelines and approved by the Institutional Animal Care and Use Committee of UC San Diego (Approval No. S09388).

CRediT authorship contribution statement

Zhongyuan Guo: Writing – original draft, Methodology, Investigation, Formal analysis, Data curation. **Audrey T. Zhu:** Methodology, Investigation. **Xiaoli Wei:** Methodology, Investigation. **Yao Jiang:** Methodology, Investigation. **Yiyan Yu:** Methodology, Investigation. **Ilkoo Noh:** Methodology, Investigation. **Weiwei Gao:** Writing – review & editing, Supervision, Conceptualization. **Ronnie H. Fang:** Writing – review & editing, Writing – original draft, Supervision, Project administration, Funding acquisition, Conceptualization. **Liangfang Zhang:** Writing – review & editing, Supervision, Funding acquisition, Conceptualization.

Declaration of competing interest

The authors declare no conflict of interest.

Acknowledgements

This work was supported by the Defense Threat Reduction Agency Joint Science and Technology Office for Chemical and Biological Defense under award number HDTRA1-21-1-0010 and the National Institutes of Health under Award Numbers R21AI159492 and R21AI175904.

References

[1] G. Schiavo, M. Matteoli, C. Montecucco, Neurotoxins affecting neuroexocytosis, Physiol. Rev. 80 (2000) 717–766.
[2] M. Pirazzini, O. Rossetto, R. Eleopra, C. Montecucco, Botulinum neurotoxins: biology, pharmacology, and toxicology, Pharmacol. Rev. 69 (2017) 200–235.
[3] A. Fulgenzi, M.E. Ferrero, EDTA chelation therapy for the treatment of neurotoxicity, Int. J. Mol. Sci. 20 (2019) 1019.
[4] H.M. Scobie, D. Thomas, J.M. Marlett, G. Destito, D.J. Wigelsworth, R.J. Collier, J. A. Young, M. Manchester, A soluble receptor decoy protects rats against anthrax lethal toxin challenge, J. Infect. Dis. 192 (2005) 1047–1051.
[5] G.J. Rainey, J.A. Young, Antitoxins: novel strategies to target agents of bioterrorism, Nat. Rev. Microbiol. 2 (2004) 721–726.
[6] K.H. Lam, J.M. Tremblay, E. Vazquez-Cintron, K. Perry, C. Ondeck, R.P. Webb, P. M. McNutt, C.B. Shoemaker, R. Jin, Structural insights into rational design of single-domain antibody-based antitoxins against botulinum neurotoxins, Cell Rep. 30 (2020) 2526–2539.e2526.
[7] A.H. Laustsen, J. Maria Gutierrez, C. Knudsen, K.H. Johansen, E. Bermudez-Mendez, F.A. Cerni, J.A. Jurgensen, L. Ledsgaard, A. Martos-Esteban, M. Ohlenschlaeger, U. Pus, M.R. Andersen, B. Lomonte, M. Engmark, M.B. Pucca, Pros and cons of different therapeutic antibody formats for recombinant antivenom development, Toxicon 146 (2018) 151–175.

[8] J.M. Rusnak, L.A. Smith, Botulinum neurotoxin vaccines: past history and recent developments, Hum. Vaccine 5 (2009) 794–805.
[9] s.w.i. World Health Organization, Electronic address, Tetanus vaccines: WHO position paper, February 2017 - recommendations, Vaccine 36 (2018) 3573–3575.
[10] E. Hammarlund, A. Thomas, E.A. Poore, I.J. Amanna, A.E. Rynko, M. Mori, Z. Chen, M.K. Slifka, Durability of vaccine-induced immunity against tetanus and diphtheria toxins: a cross-sectional analysis, Clin. Infect. Dis. 62 (2016) 1111–1118.
[11] G. Sundeen, J.T. Barbieri, Vaccines against botulism, Toxins 9 (2017) 268.
[12] C. Rasetti-Escargueil, M.R. Popoff, Antibodies and vaccines against botulinum toxins: available measures and novel approaches, Toxins 11 (2019) 528.
[13] Z.Y. Guo, L.J. Kubiatowicz, R.H. Fang, L.F. Zhang, Nanotoxoids: biomimetic nanoparticle vaccines against infections, Adv. Ther. 4 (2021) 2100072.
[14] A. Singh, Eliciting B cell immunity against infectious diseases using nanovaccines, Nat. Nanotechnol. 16 (2021) 16–24.
[15] R.H. Fang, A.V. Kroll, W. Gao, L. Zhang, Cell membrane coating nanotechnology, Adv. Mater. 30 (2018) 1706759.
[16] Z. Guo, A.T. Zhu, R.H. Fang, L. Zhang, Recent developments in nanoparticle-based photo-immunotherapy for cancer treatment, Small Methods 7 (2023) 2300252.
[17] C.M. Hu, R.H. Fang, K.C. Wang, B.T. Luk, S. Thamphiwatana, D. Dehaini, P. Nguyen, P. Angsantikul, C.H. Wen, A.V. Kroll, C. Carpenter, M. Ramesh, V. Qu, S.H. Patel, J. Zhu, W. Shi, F.M. Hofman, T.C. Chen, W. Gao, K. Zhang, S. Chien, L. Zhang, Nanoparticle biointerfacing by platelet membrane cloaking, Nature 526 (2015) 118–121.
[18] W. Gao, R.H. Fang, S. Thamphiwatana, B.T. Luk, J. Li, P. Angsantikul, Q. Zhang, C. M. Hu, L. Zhang, Modulating antibacterial immunity via bacterial membrane-coated nanoparticles, Nano Lett. 15 (2015) 1403–1409.
[19] R.H. Fang, W. Gao, L. Zhang, Targeting drugs to tumours using cell membrane-coated nanoparticles, Nat. Rev. Clin. Oncol. 20 (2023) 33–48.
[20] J. Payandeh, M. Volgraf, Ligand binding at the protein-lipid interface: strategic considerations for drug design, Nat. Rev. Drug Discov. 20 (2021) 710–722.
[21] B. Belardi, S. Son, J.H. Felce, M.L. Dustin, D.A. Fletcher, Cell–cell interfaces as specialized compartments directing cell function, Nat. Rev. Mol. Cell Biol. 21 (2020) 750–764.
[22] M. Dal Peraro, F.G. van der Goot, Pore-forming toxins: ancient, but never really out of fashion, Nat. Rev. Microbiol. 14 (2016) 77–92.
[23] Z. Guo, J. Zhou, Y. Yu, N. Krishnan, I. Noh, A.T. Zhu, R.M. Borum, W. Gao, R. H. Fang, L. Zhang, Immunostimulatory DNA hydrogel enhances protective efficacy of nanotoxoids against bacterial infection, Adv. Mater. 35 (2023) 2211717.
[24] X. Wei, J. Gao, F. Wang, M. Ying, P. Angsantikul, A.V. Kroll, J. Zhou, W. Gao, W. Lu, R.H. Fang, L. Zhang, In situ capture of bacterial toxins for antivirulence vaccination, Adv. Mater. 29 (2017) 1701644.
[25] C.M. Hu, R.H. Fang, J. Copp, B.T. Luk, L. Zhang, A biomimetic nanosponge that absorbs pore-forming toxins, Nat. Nanotechnol. 8 (2013) 336–340.
[26] D. Wang, X. Ai, Y. Duan, N. Xian, R.H. Fang, W. Gao, L. Zhang, Neuronal cellular nanosponges for effective detoxification of neurotoxins, ACS Nano 16 (2022) 19145–19154.
[27] C.M. Hu, R.H. Fang, B.T. Luk, L. Zhang, Nanoparticle-detained toxins for safe and effective vaccination, Nat. Nanotechnol. 8 (2013) 933–938.
[28] J. Zhou, N. Krishnan, Z. Guo, C.J. Ventura, M. Holay, Q. Zhang, X. Wei, W. Gao, R. H. Fang, L. Zhang, Nanotoxoid vaccination protects against opportunistic bacterial infections arising from immunodeficiency, Sci. Adv. 8 (2022) eabq5492.
[29] F. Wang, R.H. Fang, B.T. Luk, C.J. Hu, S. Thamphiwatana, D. Dehaini, P. Angsantikul, A.V. Kroll, Z. Pang, W. Gao, W. Lu, L. Zhang, Nanoparticle-based antivirulence vaccine for the management of methicillin-resistant *Staphylococcus aureus* skin infection, Adv. Funct. Mater. 26 (2016) 1628–1635.
[30] M. Holay, N. Krishnan, J. Zhou, Y. Duan, Z. Guo, W. Gao, R.H. Fang, L. Zhang, Single low-dose nanovaccine for long-term protection against anthrax toxins, Nano Lett. 22 (2022) 9672–9678.
[31] M. Holay, Z. Guo, J. Pihl, J. Heo, J.H. Park, R.H. Fang, L. Zhang, Bacteria-inspired nanomedicine, ACS Appl. Bio Mater. 4 (2021) 3830–3848.
[32] M.R. Popoff, B. Poulain, Bacterial toxins and the nervous system: neurotoxins and multipotential toxins interacting with neuronal cells, Toxins 2 (2010) 683–737.
[33] M. Dong, F. Yeh, W.H. Tepp, C. Dean, E.A. Johnson, R. Janz, E.R. Chapman, SV2 is the protein receptor for botulinum neurotoxin A, Science 312 (2006) 592–596.
[34] X. Ai, S. Wang, Y. Duan, Q. Zhang, M.S. Chen, W. Gao, L. Zhang, Emerging approaches to functionalizing cell membrane-coated nanoparticles, Biochemistry 60 (2021) 941–955.
[35] T. Ishizuka, M. Kakuda, R. Araki, H. Yawo, Kinetic evaluation of photosensitivity in genetically engineered neurons expressing green algae light-gated channels, Neurosci. Res. 54 (2006) 85–94.
[36] S. Hannan, M. Mortensen, T.G. Smart, Snake neurotoxin α-bungarotoxin is an antagonist at native $GABA_A$ receptors, Neuropharmacology 93 (2015) 28–40.
[37] A. Ledreux, S. Krys, C. Bernard, Suitability of the Neuro-2a cell line for the detection of palytoxin and analogues (neurotoxic phycotoxins), Toxicon 53 (2009) 300–308.
[38] S. Huang, S.X. Li, N. Bren, K. Cheng, R. Gomoto, L. Chen, S.M. Sine, Complex between α-bungarotoxin and an α7 nicotinic receptor ligand-binding domain chimaera, Biochem. J. 454 (2013) 303–310.
[39] S. Gu, J.A. Matta, B. Lord, A.W. Harrington, S.W. Sutton, W.B. Davini, D.S. Bredt, Brain α7 nicotinic acetylcholine receptor assembly requires NACHO, Neuron 89 (2016) 948–955.
[40] J.A. Matta, S. Gu, W.B. Davini, B. Lord, E.R. Siuda, A.W. Harrington, D.S. Bredt, NACHO mediates nicotinic acetylcholine receptor function throughout the brain, Cell Rep. 19 (2017) 688–696.
[41] J.A. Copp, R.H. Fang, B.T. Luk, C.M. Hu, W. Gao, K. Zhang, L. Zhang, Clearance of pathological antibodies using biomimetic nanoparticles, Proc. Natl. Acad. Sci. U.S. A. 111 (2014) 13481–13486.
[42] Y. Wang, Z. Wang, Y. Zhou, L. Liu, Y. Zhao, C. Yao, L. Wang, Z. Qiao, Nicotine stimulates adhesion molecular expression via calcium influx and mitogen-activated protein kinases in human endothelial cells, Int. J. Biochem. Cell Biol. 38 (2006) 170–182.
[43] S. Vijayaraghavan, P.C. Pugh, Z.W. Zhang, M.M. Rathouz, D.K. Berg, Nicotinic receptors that bind α-bungarotoxin on neurons raise intracellular free Ca^{2+}, Neuron 8 (1992) 353–362.
[44] B. Bahmani, H. Gong, B.T. Luk, K.J. Haushalter, E. DeTeresa, M. Previti, J. Zhou, W. Gao, J.D. Bui, L. Zhang, R.H. Fang, J. Zhang, Intratumoral immunotherapy using platelet-cloaked nanoparticles enhances antitumor immunity in solid tumors, Nat. Commun. 12 (2021) 1999.
[45] R. Toita, Y. Kanai, H. Watabe, K. Nakao, S. Yamamoto, J. Hatazawa, M. Akashi, Biodistribution of ^{125}I-labeled polymeric vaccine carriers after subcutaneous injection, Bioorg. Med. Chem. 21 (2013) 5310–5315.
[46] I.S. Khalek, R.R. Senji Laxme, Y.T.K. Nguyen, S. Khochare, R.N. Patel, J. Woehl, J. M. Smith, K. Saye-Francisco, Y. Kim, L. Misson Mindrebo, Q. Tran, M. Kedzior, E. Bore, O. Limbo, M. Verma, R.L. Stanfield, S.K. Menzies, S. Ainsworth, R. A. Harrison, D.R. Burton, D. Sok, I.A. Wilson, N.R. Casewell, K. Sunagar, J. G. Jardine, Synthetic development of a broadly neutralizing antibody against snake venom long-chain alpha-neurotoxins, Sci. Transl. Med. 16 (2024) eadk1867.
[47] S. Mattapally, K.M. Pawlik, V.G. Fast, E. Zumaquero, F.E. Lund, T.D. Randall, T. M. Townes, J. Zhang, Human leukocyte antigen class I and II knockout human induced pluripotent stem cell-derived cells: universal donor for cell therapy, J. Am. Heart Assoc. 7 (2018) e010239.